The Twelfth International Symposium on Magnetic Bearings (ISMB 12)
Wuhan, China, August 22-25, 2010

Self-sensing Active Magnetic Dampers for Vibration Control

Andrea Tonoli[1,a], Angelo Bonfitto[2,b], Giancarlo Genta[1,c], Mario Silvagni[2,d], Hannes Bleuler[3,e]

[1]Mechanics Department, Mechatronics Laboratory
Politecnico di Torino
Corso Duca degli Abruzzi 24, I-10129 Torino-Italy
phone: +39-0115646239 fax: +39-0115647963
http://www.cspp.polito.it
[2]Mechatronics Laboratory-Politecnico di Torino
Corso Duca degli Abruzzi 24, I-10129 Torino - Italy
phone: +39-0115646239 fax: +39 0115647963
http://www.cspp.polito.it
[3]EPFL-STI-IMT-LSRO1
Ecole Polytechnique Fédérale de Lausanne
Phone.: [+41 21 69] 35927,32565,33895,33810
[a]andrea.tonoli@polito.it, [b]angelo.bonfitto@polito.it,
[c]giancarlo.genta@polito.it, [d]mario.silvagni@polito.it,[e]hannes.bleuler@epfl.ch

Abstract: The aim of this paper is to investigate the potential of a self-sensing strategy in the case of an electromagnetic damper for the vibration control of flexible structures and rotors. The study has been performed in the case of a single degree of freedom mechanical oscillator actuated by a couple of electromagnets. The self-sensing system is based on a Luenberger observer. Two sets of parameters have been used: nominal ones (based on simplifications on the actuator model) and identified ones. In the latter case, the parameters of the electromechanical model used in the observer are identified starting from the open-loop system response. The observed states are used to close a state-feedback loop with the objective of increasing the damping of the system. The results show that the damping performance are good in both cases, although much better in the second one. Furthermore, the good correlation between the closed loop model response and the experimental results validates the modelling, the identification procedure, the control design and its implementation. The paper concludes on a sensitivity analysis, in which the influence of the model parameters on the closed-loop response is shown.

Keywords: Magnetic Dampers, Luenberger Observer, Selfsensing, Vibration Control

Introduction

Viscoelastic and fluid film dampers are the main two categories of damping devices used in machines and mechanical structures. Although cost effective and of small size and weight, they need elaborate tuning to compensate the effects of temperature and frequency. Additionally, their life is limited by fatigue and ageing, and their passive nature restricts their flexibility according to the operating conditions. Active and semiactive electrohydraulic systems have been developed in the past to allow some forms of online tuning or adaptive behavior. More recently, electrorheological [1,2] and magnetorheological [3] semiactive damping systems have shown attractive potential for the adaption of the damping force to the operating conditions. However, electrohydraulic, electrorheological, and magnetorheological devices cannot avoid some drawbacks related to the ageing of the fluid and to the tuning required for the compensation of the temperature and frequency effects.

Electromechanical dampers seem to be a valid alternative to viscoelastic and hydraulic ones due to, among the others, (a) the absence of all fatigue and tribology issues motivated by the absence of contact, (b) the smaller sensitivity to the operating conditions, (c) the wide possibility of tuning even during operation, and (d) the predictability of the behavior. The attractive potential of electromechanical damping systems motivated a considerable research effort for the past decade. The target applications range from the field of rotating machines to that of vehicle suspensions [4,5].

In principle, the difference between active magnetic bearings (AMB) and dampers (AMD) is rather small. In the former case (AMB), the shaft is completely supported by electromagnets, which achieve levitation and vibration control at the same time. In the latter case (AMD), the rotor is supported by mechanical means, and the electromagnetic actuators are used only to control the shaft vibrations.

The combination of a mechanical suspension with an electromagnetic actuator is advantageous for two main reasons: the system can be designed to be stable even in open loop and the actuators are smaller [6,7,8] relative to the AMB configuration. As a matter of fact, the issue is no longer the realization of the suspension, but rather to control mechanical vibrations.

It is well known that in a AMB the control system must compensate the intrinsically unstable behavior due to the negative stiffness induced by the electromagnets. The adoption of a mechanical stiffness in parallel to the electromagnets allows to compensate this negative stiffness making the system stable even in open loop.

As a consequence of that, the only task of the closed loop control is the introduction of damping in the system.

Damping may be introduced into the structure by simply feeding back the position-sensor signal by means of a proportional-derivative controller. This approach has all the promising aspects of AMBs, as unbalance compensation, faults detection, and so on. In addition to the active solutions, passive or semi-active solutions are also possible. They can be obtained by connecting the electromagnets to constant voltage power supply. In this case, the mechanical energy is dissipated by the eddy currents that develop into the electromagnets' coils due the relative motion of the anchor [9]. In the active, passive and semi-active case, the open-loop stability is insured as long as the mechanical stiffness compensates the negative stiffness introduced by the electromagnetic actuator.

The reversibility of the electromechanical interaction induces an electrical effect when the two parts of an electromagnet are subject to relative motion (back electromotive force). This effect can be exploited to estimate mechanical variables from the measurement of electrical ones. This leads to the so-called self-sensing configuration that consists in using the electromagnet either as an actuator and a sensor. This configuration permits lower costs and shorter shafts (and thus higher bending frequencies) than classical AMB configurations, and non-collocation issues are avoided.

In practice, voltage and current are used to estimate the airgap. To do so, the two main approaches are: the state-space observer approach [10,11] and the airgap estimation using the current ripple [12,13].

The former is based on the electromechanical model of the system. As the resulting model is fully observable and controllable, the position and the velocity of the mechanical part can be estimated and fed back to control the vibrations of the system. This approach is applicable for voltage-controlled [14] and current-controlled [15] electromagnets.

The second approach takes advantage of the current ripple due to the switching amplifiers to compute in real-time the inductance, and thus the airgap. The airgap-estimation can be based on the ripple slope (PWM-driven amplifiers, [16] or on the ripple frequency (hysteresis amplifiers, [17].

So far in the literature, self-sensing configurations have been mainly used to achieve the complete suspension of the rotor. The poor robustness of the state-space approach greatly limited its adoption for industrial applications. As a matter of fact, the use of a not well tuned model results in the system instability [14,18]. Instead, the direct airgap estimation approach seems to be more promising in terms of robustness [19].

In the authors' knowledge, the application of the self-sensing approach to AMDs have not been reported in the literature yet, although this configuration is promising regarding the robustness. In fact, the presence of errors in the model used for the control synthesis has less impact on the system integrity than for AMBs, given that the mechanical suspension stabilizes the system. In the worst case, reasonable deviations from the nominal model only lead to lower damping performance, instead of instability as it is the case for AMBs. Therefore, from this point of view, larger robustness is obtained for this configuration.

The aim of the present paper is to investigate the potential of the self-sensing approach in the case of AMD configurations. To this end, an observer-based control is developed to damp the vibrations of a single degree of freedom system provided with an electromagnetic actuator. The observer is based on the linearized model of the mechanical plant. The parameters of this model can be obtained in two different ways.

In the first case, the model is built under the assumption that the actuator material has infinite magnetization, no magnetic saturation and no air gap leakage. Therefore, the expression of the inductance can be used to compute the different electromechanical factors, such as the back-electromotive force factor, the current-to-force factor and the negative stiffness. The resulting model is then used to compute the observer and the controller.

In the second case, the model parameters are identified through a model-based procedure. Owing to the intrinsic stability of the system, the identification is relatively easy to perform. As this approach gives a more precise model, it obtains better damping performance.

The experimental results of the controller based on the nominal and identified models are exposed, and the identification procedure is validated. It is shown that a good damping performance is obtained in both configurations, although the damping performance of the controller based on the identified model is higher, as expected. Consequently, the paper ends with the sensitivity analysis of the control performance with respect to the variation of the system parameters.

Modelling and experimental setup

The considered system is a one degree of freedom mass-spring oscillator actuated by two opposite electromagnets, corresponding to an AMD configuration, as shown in Fig. 1. Parameters m , k and c are the mass, stiffness and viscous damping coefficient of the mechanical system, respectively.

The electromagnets are assumed to be identical, and the coupling between the two electromagnetic circuits is neglected. The aim of the mechanical stiffness is to compensate the negative stiffness due to the electromagnets.

The electromagnets are assumed to be identical, and the coupling between the two electromagnetic circuits is neglected.

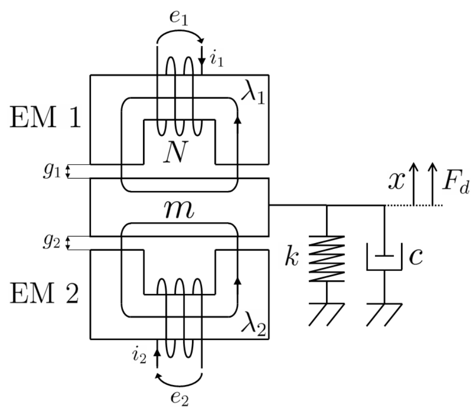

Figure 1: Model

Each electromagnet can be considered as a two-port element (electrical and mechanical). The force generated by each electromagnet is expressed as

$$F_j(i_j, x) = \frac{\partial E_j(i_j, x)}{\partial x}, \qquad j = 1,2 \tag{1}$$

Where E_j is the energy stored in the electromagnet j and x is the displacement.

The action of the electromagnets has been linearized around the working point and then the whole model containing the mechanical and electromechanical subsystems has been expressed as a three state state-space system:

$$\begin{aligned} \dot{X} &= AX + Bu \\ y &= CX \end{aligned} \tag{2}$$

where A, B, C are the dynamic, action and output matrices, respectively, defined as:

$$A = \begin{bmatrix} 0 & 1 & 0 \\ -\dfrac{k + 2k_x}{m} & -\dfrac{c}{m} & \dfrac{2k_i}{m} \\ 0 & -\dfrac{k_m}{L_0} & -\dfrac{R}{L_0} \end{bmatrix}$$

$$B = \begin{bmatrix} 0 & 0 \\ \dfrac{1}{m} & 0 \\ 0 & \dfrac{1}{L_0} \end{bmatrix}, \; C = \begin{bmatrix} 0 & 0 & 1 \end{bmatrix} \tag{3}$$

with the associated input and output state vectors $X = \left\{ x, \dot{x}, i_c \right\}^T$, $u = \{F_d, e_c\}^T$ and $y = i_c$.

The terms $L_0, k_{i,} k_m$ and k_x are the inductance, the current-force factor, the back-electromotive force factor and the so-called negative stiffness of one electromagnet, respectively.
The system used for the experimental investigation is a test rig available at the Mechatronics Laboratory of Politecnico di Torino presented in Fig. 2 and in Fig. 3. It is used for static characterization of radial magnetic bearings and to analyze different control strategies, sensors and power amplifiers in a simple and well-known experimental set-up without the need of an expensive prototype of the whole suspension.

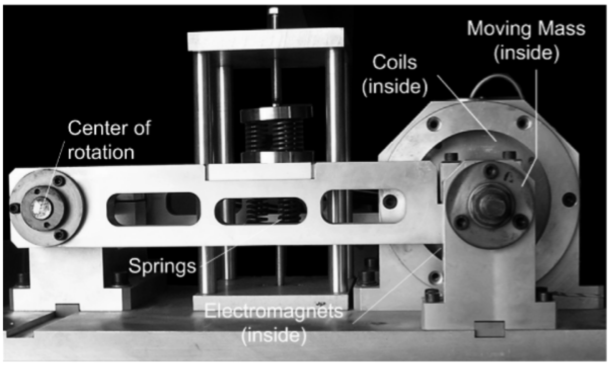

Figure 2: Photo of the test rig

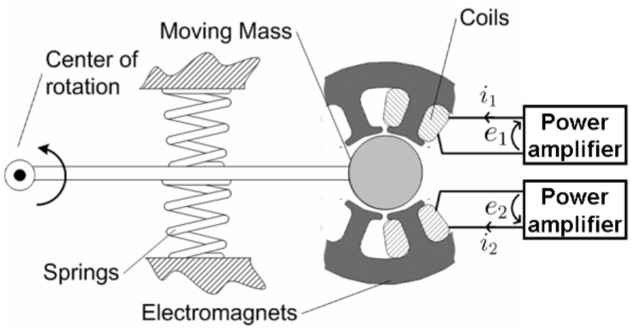

Figure 3: Test rig scheme

This rig consists in a horizontal arm hinged at one extremity with a pivot, and actuated with a single axis magnetic bearing. The electromagnets have 142 windings, an airgap area $S = 4.2 \cdot 10^{-4} m^2$, and a nominal airgap of approximately $x_0 = 0.6mm$. The length of the pendulum (320 mm) compared to the nominal airgap insures that the circular motion of the mass can be approximated with a linear translation (x). The base plate, connecting arms and electromagnets' housing are made of aluminium, while the shafts are made of steel. The ferromagnetic circuit (stator and moving part) of the electromagnet is made of silicon iron sheets. Six springs in parallel are located at a distance of 160 mm from the hinge to provide a stabilizing stiffness to the system.
A DSP TI TMS320F2812 integrated in the ACTUA EKU 2.1 control board has been used for the control implementation. The Analog-to-Digital converters use 12 bit over a range of 3V, with a sampling rate of 4.5kHz.
The position was measured with a Bently Proximitor 3300XL eddy current sensor just for monitoring and validation, and not for feedback purposes. AMP25 Hall current sensors

(range $\pm 5A$) were used for the current measurement in the two coils (lower than 100mA, peak-to-peak, of noise).
The DC value of the PWM power amplifier was set to 20~ V, and the switching frequency was set to 36.6kHz. Thus, as both the sampling rate and the switching frequency of the PWM were far beyond the mechanical frequency of the system (around 20 Hz), their dynamics was neglected during the study.
Two sets of parameters have been used to build the models from which was computed the observer/controller.
The first set is based on the simplified expression of the inductance, i.e. $L(x) = \dfrac{\Gamma}{x_0 \mp x}$, from which the other electromechanical parameters were obtained. Those values are reported in Table 1 (parameter c is negligible if compared to the damping introduced by the electromechanical effect).
The second set of parameters have been identified experimentally under two assumptions:

- k , c and m are determined from physical dimensions, direct measurements and from impact response in open-circuit electromagnets conditions;
- the electro-mechanical parameters k_m and k_i are equal.

The parameters of the identified model are presented in Table 1.
Fig. 4 presents the comparison between the experimental admittance and the admittance obtained from the nominal model (dotted line) and the identified model (dashed line). The good correlation between the experimental and identified plots validates the proposed procedure.

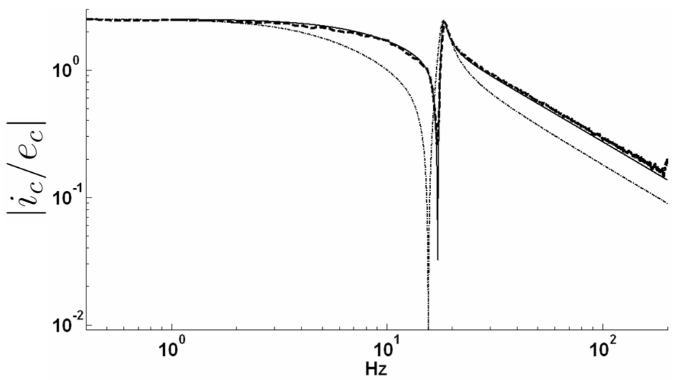

Figure 4: Voltage to current transfer function (admittance). Solid and dashed lines are the identified model and the plant admittance, respectively. The dotted line represents the admittance evaluated by means of the nominal expression of the inductance ($L_0 = \dfrac{\Gamma}{x_0}$)

Control Design

The aim of the present section is to describe the design strategy of the controller that has been used to introduce active magnetic damping into the system. In this paper, the control is based on the Luenberger observer approach. The adoption of this approach was motivated by the relatively low level of noise affecting the current measurement. It consists in estimating in real time the unmeasured states (in our case, displacement and velocity) from the processing of the measurable states (the current). The observer is based on the linearized model presented in Section “Modeling and experimental setup”, and therefore the higher frequency modes of the mechanical system have not been taken into account. Afterwards, the same model is used for the design of the state-feedback controller.

Table1: Model parameters

Symbol	Value		Unit
Mechanical parameters			
k	46.5		kN/m
m	3.42		kg
c	≈ 0		$N.s/m$
Electrical parameters			
R	0.4		Ω
	Nominal	Identified	
L_0	8.9	5.8	mH
k_i	7.39	3.96	N/A
k_m	7.39	3.96	Vm/s
k_x	-6.16	-3.3	kN/m

State observer. The observer dynamics is expressed as [20]:

$$\dot{\hat{X}} = A\hat{X} + Bu + L(y - \hat{y}). \tag{4}$$

where $\hat{x}$ and $\hat{y}$ are the estimation of the system states and outputs, respectively. Matrix L is commonly referred to as the gain matrix of the observer. The inputs (y) of the observer are the measurement of the current and the control voltage on the electromagnets (u).
The dynamics of the estimation error ε are obtained as follows:

$$\dot{\varepsilon} = (A - LC)\varepsilon \tag{5}$$

where $\varepsilon = X - \hat{X}$. Equation (5) emphasizes the role of L in the observer convergence. The location of the eigenvalues of matrix $A - LC$ on the complex plane determines the estimation time constants of the observer: the deeper they are in the left-half part of the complex plane, the faster will be the observer. It is well known that the observer tuning is a trade-off between the convergence speed and the noise rejection [20]. A fast observer is desirable to increase the frequency bandwidth of the controller action. Nevertheless, this configuration corresponds to high values of L gains, which would result in the amplification of the unavoidable measurement noise y, and its transmission into the state estimation. This issue is especially relevant when switching amplifiers are used. Moreover, the transfer

function that results from a fast observer requires large sampling frequencies, which is not always compatible with low cost applications.
In this work, a classical pole placement has been performed to determine the gains of matrix L. They have been chosen such that the eigenvalues of $A-LC$ have the same imaginary parts of the eigenvalues of A (p_1, p_2 and p_3), while their real parts are multiplied by a factor of 30 for the conjugate complex poles (p_1 and p_2), and 10 for the real pole (p_3). The performance of the resulting observer was then estimated in simulation to check that all requirements concerning convergence speed, noise and sampling issues were met.

State-feedback controller. A state-feedback control is used to introduce damping into the system. The control voltage is computed as a linear combination of the states estimated by the observer, with K as the control gain matrix. Owing to the separation principle, the state-feedback controller is designed considering the eigenvalues of matrix $A-BK$.
Similarly to the observer, a pole placement technique has been used to compute the gains of K, so as to maintain the mechanical frequency constant. By doing so, the power consumption for damping is minimized, as the controller does not work against the mechanical stiffness. The idea of the design was to increase damping by shifting the complex poles closer to the real axis while keeping constant their distance to the origin.
The separation principle implies that the overall closed-loop dynamics is then given by the observer poles and the state-feedback controller poles ($eig(A-LC)$ and $eig(A-BK)$. Nevertheless, only the dominant poles are considered to characterize the damping characteristics of the system. In the present case, the control strategy increases the damping factor ξ of the system from $\xi_{OL}=0.03$ (Open-loop) to $\xi_{CL}=0.3$ (Closed-loop). The presented results refer to the model computed from the identified parameters.

Experimental results

The open-loop voltage-to-displacement transfer function obtained from the model and the experimental tests are compared in Fig. 5. The correspondence between the two plots is considered as a good validation of the modelling and identification approach.
The same transfer functions in closed-loop operation with the controller designed in Sec. “Control design” are compared in Fig. 6 in the case of identified parameters. Also in this case, the correspondence is quite good, which corroborates the control approach, and validates the whole procedure.

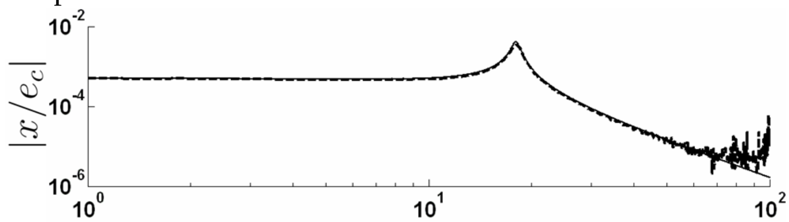

Figure 5: Frequency response of the test rig in open-loop configuration, and comparison with the model. Solid and dashed lines are the model and the plant frequency responses, respectively.

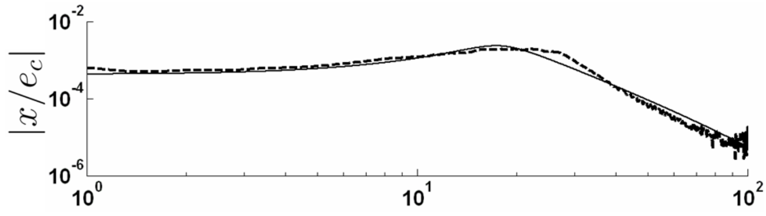

Figure 6: Frequency response of the test rig in closed-loop configuration, and comparison with the model. Solid and dashed lines are the model and the plant frequency responses, respectively.

The damping performance is evaluated by analyzing the time response of the closed-loop system when an impulse excitation is applied to the system. The impulse excitation is obtained by hitting the system with a hammer.

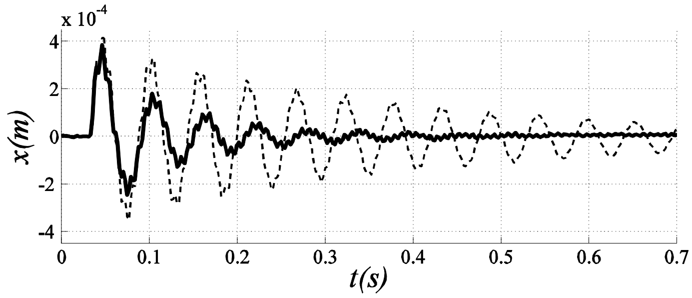

Figure 7: Time response of the test rig to an impulse excitation. The time response of the system in two different configurations is plotted as follows: open-loop (dashed line) and closed-loop based on the nominal inductance (solid line)

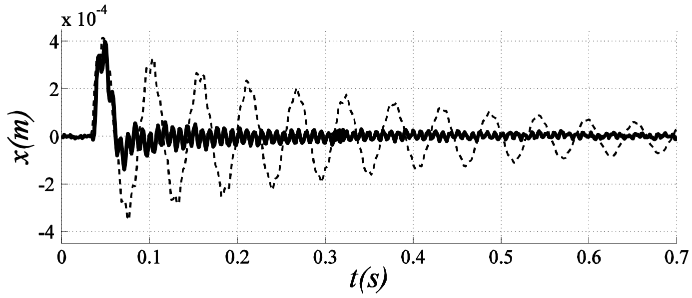

Figure 8: Time response of the test rig to an impulse excitation. The time response of the system in two different configurations is plotted as follows: open-loop (dashed line) and closed-loop based on the identified model (solid line)

In Fig. 7, the open-loop system response (dashed line) is compared to the closed-loop one when the observer and state-feedback controller are designed from a model based on the nominal value of the system parameters.
In Fig. 8, the open-loop system response (dashed line) is compared to the closed-loop one when the observer and state-feedback controller are designed from a model based on the identified values of the system parameters.
As expected, it can be seen that the controller based on the identified electromechanical parameters give better results than the nominal model. However, it can be emphasized that

the damping performance of the controller based on the nominal model is still convincing. This result is worthy, as it shows that good damping can be conveniently achieved for active magnetic dampers obtained with the simplified model. Furthermore, this controller does not destabilize the system, as it is the case for full suspension self-sensing configurations.
In the following, a sensitivity analysis is performed to quantify the influence on the control performance of the deviation of the model parameter from those identified experimentally.

Sensitivity analysis

The closed-loop performance of the system is affected by the error between the estimated and the "real" states. The larger are these errors, the poorer is the control performance. The estimation error depends on the accuracy of the parameters of the model adopted for the estimator design.
The objective of this section is to study the influence on the closed-loop performance of the parameters deviation from the identified values of the model. This analysis is motivated by the common knowledge that state-observer strategies for self-sensing magnetic bearings have poor robustness [14], as far as the complete suspension of the system is concerned, as it is done in literature.
This analysis is focused on the influence of the variation of the parameters defined in Table 1 on the dynamics of the closed-loop system. The procedure consists in freezing the controller designed from the identified model, while the plant parameters, namely k_x, k_m, L_0, R, k and m, are modified individually in order to single out the most relevant ones. As it could have been expected, the critical parameters are the resistance R, the nominal inductance L_0 and the mechanical stiffness k, henceforth, only the root loci that correspond to the variation of those parameters are presented in Fig. 9. Each parameter has been modified incrementally from the minimum value that drives the closed-loop system to instability up to twice the identified value (higher values of the parameters are not realistic).
It can be seen in Fig. 9 (a) that the closed-loop system is unstable for values lower than 0.22 Ohm, and remains stable for values much larger than 0.8 Ohm.
Similarly, the variation of the inductance, as shown in Fig. 9(b), indicates that the closed-loop system is unstable for values lower than 4.9 mH, and remains stable for values much larger than 11.6 mH.

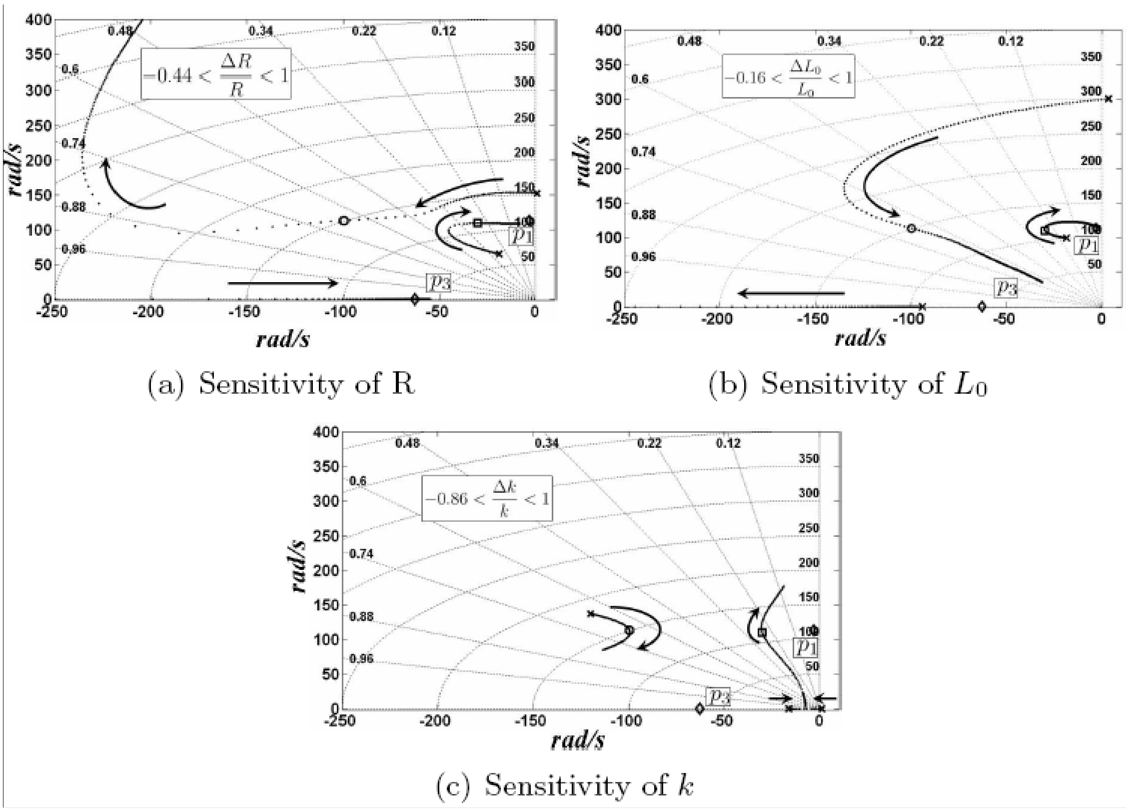

(a) Sensitivity of R

(b) Sensitivity of L_0

(c) Sensitivity of k

Figure 9: Sensitivity analysis. × corresponds to the closed-loop poles associated to the model modified with the smallest relative error leading to instability. ◊ symbol refers to the open-loop system poles, while ○ and □ refer to the observer $A - LC$ and the state-feedback controller $A - BK$ poles with the identified model, respectively.

In the case of the variation of the stiffness (Fig. 9 (c)), the closed-loop system is unstable for values lower than 6.51kN/m, and remains stable for values much larger than 93 kN/m, which corresponds to. The closed-loop poles are real until they become complex conjugate.
The sensitivity analysis emphasizes that for plants whose stiffness, resistance and inductance parameters are larger than those of the identified one, the closed-loop system remains stable, although with reduced damping performance. This conclusion confirms the result presented in Fig. 7 and in Fig. 8, in which it is clear that the damping performance of the controller based on the nominal model is lower than the one of the identified model. This remark can be used as a hint to find a reasonably safe approach for the design of a self-sensing AMD, without performing an exhaustive robustness analysis. In fact, one might think of a controller based on a model whose parameters are lower than those of the plant, such that the overall stability is insured. Furthermore, the hypothetical variation of the plant in working conditions (such that the resistance and the mechanical stiffness, for instance) could also be taken into account, insuring stability at the cost of the damping performance.

Conclusions

The study of an observer-based self-sensing active magnetic damper has been presented both in simulation and experimentally. The objective of the work was to investigate the potential and critical aspects of self-sensing controllers for dampers instead of active magnetic bearing applications. It has been shown that the damping performance of the Luenberger observer-based approach are comparable to the control strategies based on the position sensor feedback. Two sets of parameters have been used to build the observer/controller systems: one based on the simplified expression of the inductance, and one based on an identification approach. The former allows a synthesis of the observer/controller using the known parameters of the actuator (number of wires and the air gap area), and the results are quite promising. In fact, despite the simplifications implied by this approach, the closed-loop system has good damping performances. Furthermore, an identified model has been built, taking advantage of the inherent stability of this configuration. To this end, an identification procedure has been proposed. The observer and the state-feedback controller design based on the identified model has been presented. The modelling approach and the identification procedure have been validated experimentally comparing the open-loop and the closed-loop frequency response to the model. A sensitivity analysis based on the deviation from the identified parameters has been exposed, and the root loci charts have been presented for the most critical parameters, i.e. the resistance, the inductance and the mechanical stiffness. It has been shown the self-sensing configuration provides good robustness performances even for relatively large parameter deviations.

References

[1] Ahn, Y., Yang, B.-S., and Morishita, S., 2002, ``Directional controllable squeeze film damper using electro-rheological fluid," ASME J. Vibr. Acoust., 124, pp. 105-109.

[2] Vance, J. M., and Ying, D., 2000, ``Experimental measurements of actively controlled bearing damping with an electrorheological fluid," ASME J. Eng. Gas Turbines Power, 122 (2), pp. 337-344.

[3] Carmignani, C., Forte, P., and Rustighi, E., 2004, ``A fuzzy control for a magnetorheological squeeze-film damper," Proceeding of the International conference on noise and vibration engineering, (ISMA), 20-22 Sept., Leuven, Belgium, pp. 187-200..

[4] Kasarda, M., Johnson, M., Imlach, J., Mendoza, H., Kirk, G., and Bash, H., 2000, ``Applications of a magnetic bearing acting as an actuator in conjunction with conventional support bearings," Proceedings of the Ninth International Symposium on Magnetic Bearings, University of Kentucky, 3-6 Aug., Lexington, KY, pp. 1-6.

[5] Vance, J. M., Ying, D., and Nikolajsen, J. L., 2000, ``Actively controlled bearing dampers for aircraft engine applications," ASME J. Eng. Gas Turbines Power, 122 (3), pp. 466-472.

[6] Genta, G., Tonoli, A., Amati, N., Macchi, P., Silvagni, M., and Carabelli, S., 2006, ``More electric aeroengines: tradeoff between different electromagnetic dampers and supports," Tenth International Symposium on Magnetic bearings, EPFL, 21-23 Aug., Martigny, Switzerland.

[7] Amati, N., Carabelli, S., Macchi, P., Silvagni, M., and Tonoli, A., 2006, ``Transformer eddy current dampers for the vibration control of rotating machines," Eighth biennal ASME Conference on engineering system design and analysis, 4-7 July, Turin, Italy.

[8] Genta, G., Festini, A., De L\'{e}pine, X., 2008, ``From oil to magnetic fields: active and passive vibration control," Acta mechanica et automatica, 2(2), pp. 11-20.

[9] Tonoli, A., Amati, N., Silvagni, M., 2008, ``Transformer eddy current dampers for the vibration control," J. Dyn. Syst., Meas., Cont., 130, pp. 031010-1 - 031010-9.

[10] Vischer, D., and Bleuler, H., 1990, ``A new approach to sensorless and voltage controlled AMBs based on network theory concepts," Second International Symposium on Magnetic bearings, 12-14 July, Tokyo, Japan, pp. 301-306.

[11] Vischer, D., and Bleuler, H., 1993, ``Self-sensing magnetic levitation," IEEE Trans. on Magn., 29(2), pp. 1276-1281.

[12] Noh, M. D., and Maslen, E. H., 1997, ``Self-sensing magnetic bearings using parameter estimation," IEEE Trans. Instr. Meas., 46(1), pp. 45-50.

[13] Schammass, A., Herzog, R., Buhler, P., and Bleuler, H., 2005, ``New results for self-sensing active magnetic bearings using modulation approach," IEEE Trans. Contr. Syst. Tech., 13(4), pp. 509-516.

[14] Mizuno, T., Araki, and K., Bleuler, H., 1996, ``Stability analysis of self-sensing magnetic bearing controllers," IEEE Trans. Contr. Syst. Tech., 4(5), pp. 572-579.

[15] Mizuno, T., Namiki, H., and Araki, K., 1996, ``Self-sensing operations of frequency-feedback magnetic bearings," Fifth International Symposium on Magnetic Bearings, 29-30 Aug., Kanazawa, Japan, pp. 119-123.
[16] Okada, Y., Matsuda, K., and Nagai,B., 1992, ``Sensorless magnetic levitation control by measuring the PWM carrier frequency component," Third International Symposium on Magnetic Bearings, 21-31 July, Radisson Hotel, Alexandria, VA.
[17] Mizuno, T., Ishii, T., and Araki, K., 1998, ``Self-sensing magnetic suspension using hysteresis amplifier," Cont. Eng. Pract., 6, pp. 1133-1140.
[18] Thibeault, N. M., Smith, R., 2002, ``Magnetic bearing measurement configurations and associated robustness and performance limitations," J. Dyn. Syst., Meas. Contr., 124, pp. 589-598.
[19] Maslen, E., H., Montie, D., T., Iwasaki, T., 2006, ``Robustness limitations in self-sensing magnetic bearings," J. Dyn. Syst., Meas. Contr., 128, pp. 197-203.
[20] Luenberger, D. G., 1971, ``An introduction to observers," IEEE Trans. Autom. Contr, AC-16(6), pp. 596-602.